ISSN 1063-7834, Physics of the Solid State, 2013, Vol. 55, No. 11, pp. 2368–2373. © Pleiades Publishing, Ltd., 2013.
Original Russian Text © A.E. Galashev, V.A. Polukhin, 2013, published in Fizika Tverdogo Tela, 2013, Vol. 55, No. 11, pp. 2250–2255.

SURFACE PHYSICS AND THIN FILMS

Computer Simulation of Thin Nickel Films on Single-Layer Graphene

A. E. Galashev[a, *] and V. A. Polukhin[b]

[a] *Institute of Industrial Ecology, Ural Branch of the Russian Academy of Sciences, ul. Sofii Kovalevskoi 20, Yekaterinburg, 620219 Russia*

** e-mail: galashev@ecko.uran.ru*

[b] *Institute of Material Studies and Metallurgy, Ural Federal University named after the First President of Russia B. N. Yeltsin, ul. Mira 19, Yekaterinburg, 620002 Russia*

Received April 16, 2013

Abstract—The energy, mechanical, and transport properties of nickel films on a single-layer graphene sheet in the temperature range 300 K ≤ T ≤ 3300 K have been investigated using the molecular dynamics method. The stresses generated in the plane of the metallic film are significantly enhanced upon deposition of another nickel film on the reverse side of the graphene sheet. In this case, the self-diffusion coefficient in the film plane above 1800 K, in contrast, decreases. An appreciable temperature elongation per unit length of the film also occurs above 1800 K and dominates in the "zigzag" direction of the graphene sheet. The vibrational spectra of the nickel films on single-layer graphene for horizontal and vertical displacements of the Ni atoms have very different shapes.

DOI: 10.1134/S1063783413110085

1. INTRODUCTION

The interface between graphene and a metallic substrate is of great importance for the use of graphene in integrated electronics, as heat-insulating materials, and in electromechanical devices, including those for protecting their microscopic units from aggressive environmental factors. A promising method for producing large graphene areas [1–3] is the catalytic decomposition of hydrocarbons on a hot metallic surface. The possibility of chemical dissolution of a metallic substrate, after the growth of graphene has been completed, provides a means for producing free graphene sheets, which, subsequently, can be transferred to any other substrate. Nickel is a typical catalyst for the growth of nanotubes and materials used in the formation of graphene [4]. Carbon atoms are easily dissolved in nickel with the formation of an ordered metastable phase of nickel carbide Ni_2C on the surface [5, 6]. The formation of this coating (Ni_2C) with a thickness of one atomic layer competes with the growth of graphene. In the fabrication of electronic circuits, it is particularly important to obtain graphene directly on the working surface. The Ni_2C coating is formed by thermal decomposition of hydrocarbons at low temperatures, whereas graphene is predominantly formed at higher temperatures between 750 and 980 K. At still higher temperatures, carbon diffuses deep into the coating.

It is known that transition metal nickel has been used for the preparation of graphene by means of evaporation and subsequent precipitation of carbon atoms. A method for producing graphene that does not require heating of the material components to temperatures in the range of 1300 K was proposed in [7]. Therefore, the synthesis of graphene can be performed on a substrate of the material that is not capable of withstanding an intense heating. The essence of this technique lies in that, after drying a nickel–graphite film, a part of carbon atoms diffuse through natural channels under the nickel component of the film and form a monoatomic layer, i.e., graphene. Then, the upper layers are removed by the chemical method. Thus, the investigation of the physical properties of the contact of a thin nickel film with graphene at high temperatures is of both scientific and practical importance.

The purpose of this work was to investigate the energy, mechanical, and transport properties of thin nickel films brought into contact with single-layer graphene, as well as to analyzed the influence of these films on the temperature dependence of the energy of graphene.

2. COMPUTER MODEL

The calculations were performed by the classical molecular dynamics method. In this study, we used three types of empirical potentials describing the carbon–carbon (in graphene), nickel–nickel, and nickel–carbon interactions. The representations of the interactions in graphene were based on the use of the Tersoff potential [8, 9]. This potential was successfully tested on many single- and multicomponent systems with covalent chemical bonding [10, 11]. However, the transition to the simulation of two-dimen-

sional systems (for example, graphene) with covalent bonding revealed some difficulties in using this potential. The main disadvantages were as follows: the interaction was represented only by short-range covalent forces, and the contributions from the interactions with neighbors of the second and higher orders were not considered. The simulation with this potential led to cracking the graphene sheet even at low temperatures. Another serious disadvantage was in the existence of the net torsional moment appearing because of the lack of mutual compensation of the torsional moments determined by bonds around each atom. As a result, there occurred rotation of the graphene sheet (most frequently, counterclockwise). This effect impeded simulation of nanocomposites and made difficult structural analysis. In the proposed model, the aforementioned disadvantages were eliminated as follows. The scale of covalent interaction in the model was increased from 0.21 to 0.23 nm. Outside the covalent interaction, we used a very weak attractive Lennard-Jones interaction with the parameters taken from [12]. To prevent rotation of the graphene sheet, the "retardation" at each atomic site of the graphene atomic was provided by the force $-dV_{ij}(\Omega_{kijl})/dr_{ij}$, where the torsional potential $V_{ij}(\Omega_{kijl})$ is represented by the expression [13]

$$V_{ij}^{\text{tors}}(\Omega_{kijl}) = \varepsilon_{kijl}\left[\frac{256}{405}\cos^{10}\left(\frac{\Omega_{kijl}}{2}\right) - \frac{1}{10}\right], \quad (1)$$

and the torsion angle Ω_{kijl} is defined as the angle between the planes, of which one plane is specified by the vectors $\mathbf{r}_{ik}$ and $\mathbf{r}_{ij}$, and the other plane, by the vectors $\mathbf{r}_{ij}$ and $\mathbf{r}_{jl}$:

$$\cos\Omega_{kijl} = \frac{\mathbf{r}_{ji}\times\mathbf{r}_{ik}}{|\mathbf{r}_{ji}\times\mathbf{r}_{ik}|}\frac{\mathbf{r}_{ij}\times\mathbf{r}_{jl}}{|\mathbf{r}_{ij}\times\mathbf{r}_{jl}|}. \quad (2)$$

The height of the barrier ε_{kijl} for the rotation was taken from [12].

The interaction between the Ni atoms was specified by the many-body Sutton–Chen potential [13], and the interaction of the C and Ni atoms was described by the Morse potential with the parameters fitted by the density functional theory method [14].

The stress at the site of the ith atom of the metallic film is defined as [13]

$$\sigma_{\alpha\beta}(i) = \frac{\varepsilon}{2a^2\Omega_i}\sum_{i\neq j}^{k}[-n(a/r_{ij})^{n+2} + mc(1/\sqrt{\rho_i} + 1/\sqrt{\rho_j})(a/r_{ij})^{m+2}]r_{ij}^{\alpha}r_{ij}^{\beta}, \quad (3)$$

where ε is the parameter with the dimension of energy; c is the dimensionless parameter; $\rho_i = \sum_{j\neq i}(a/r_{ij})^m$; a is the parameter with the dimension of length, which is usually chosen equal to the lattice constant; m and n are positive integers ($n > m$); and the volume corresponding to an individual atom Ω_i can be associated with the volume of the Voronoi polyhedron related to the ith atom.

The initial packing of Ni atoms was represented by a monolayer in the form of a loose (111) plane of the face-centered cubic (fcc) lattice (parallel to the graphene plane) with the distance between the nearest neighbor atoms $r_{\text{Ni–Ni}} = 0.6336$ nm. In this case, the Ni atoms were arranged directly against the centers of hexagonal cells formed by carbon atoms, and the shortest distance between the C and Ni atoms $R_{\text{C–Ni}} = 0.2018$ nm corresponded to $r_{\text{C–Ni}}$ calculated in terms of the density functional theory [15]. In the bulk nickel crystal, $R_{\text{Ni–Ni}} = 0.2489$ nm. Therefore, the Ni film was initially in a stretched state due to the lattice mismatch between graphene and nickel. The shortest distance between the C atoms in graphene was $r_{\text{C–C}} = 0.142$ nm. In addition to system I, where the nickel film was located above the graphene sheet, we also considered system II with two identical symmetrically arranged nickel films with respect to the graphene sheet. The equations of motion were integrated by the fourth-order Runge–Kutta method with a time step $\Delta t = 0.2$ fs. The duration of the calculation for each temperature was $10^6\Delta t$ or 200 ps. The calculations were started at a temperature of 300 K. After every million of time steps, the temperature of the system was increased by 500 K, and the following calculation of the same duration was carried out. The last calculation corresponded to a temperature of 3300 K. The temperature in the model was maintained by the Berendsen thermostat [16].

3. RESULTS OF THE CALCULATION

The configuration of graphene at a temperature of 1300 K, covered from the top and bottom with nickel, is shown in Fig. 1. Nickel atoms in the upper layer are arranged in the form of a dense drop, whereas the metal atoms located below the graphene sheet are spread so that part of them adheres to the graphene sheet and the other part is substantially distanced from it. Some of the lower Ni atoms are outside the xy boundaries determined by the graphene sheet. A part of these atoms moves upward past the graphene sheet.

The potential energies of the interactions nickel–nickel $U_{\text{Ni–Ni}}$, nickel–carbon $U_{\text{Ni–C}}$, and carbon–carbon $U_{\text{C–C}}$ for systems I and II are shown in Fig. 2. The initial arrangement of the metal atoms on graphene does not correspond to a stable crystalline state, because the Ni atoms are located at a considerable distance from each other. An increase in the temperature and the associated enhancement in the mobility of the Ni atoms lead to the structural relaxation of the metallic film. Consequently, we should expect a decrease in the potential energy for the nickel–nickel interactions with the initial increase in the temperature, which was actually observed in both cases. The potential energy $U_{\text{Ni–Ni}}$ decreased already at a temperature of 800 K in

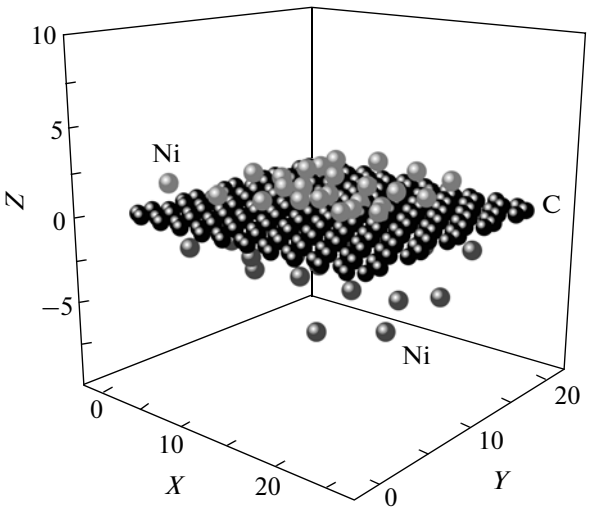

Fig. 1. Configuration of the graphene–nickel system with a two-sided arrangement of Ni atoms on the graphene sheet at an instant of time of 200 ps and at a temperature of 1300 K. The atomic coordinates are in given in angstroms.

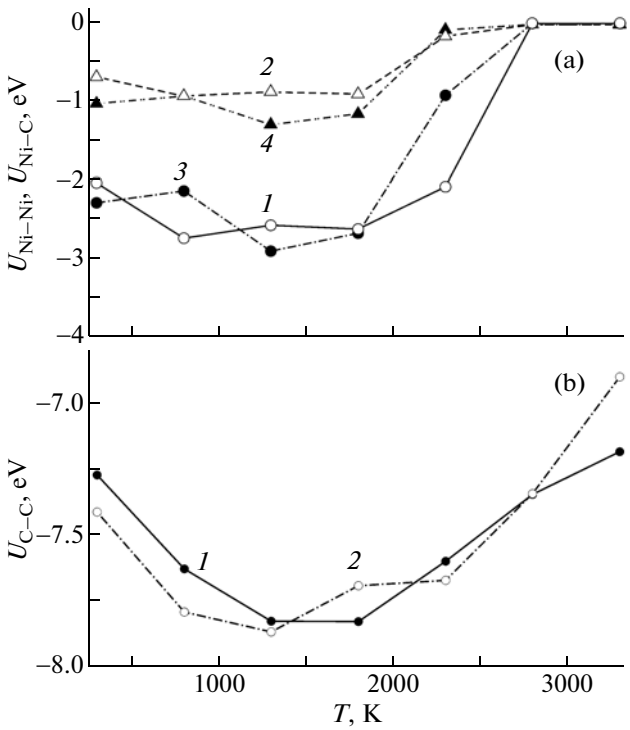

Fig. 2. (a) Partial potential energies (*1*, *3*) U_{Ni-Ni} and (*2*, *4*) U_{Ni-C} for different systems: (*1*, *2*) Ni film on one side of the graphene sheet and (*3*, *4*) Ni film on both sides of the graphene sheet. (b) Potential energy U_{C-C} for (*1*) free graphene sheet and (*2*) graphene sheet covered by the Ni film on one side or on both sides.

the presence of one metallic film on graphene, whereas in the presence of two metallic films, the value of U_{Ni-Ni} decreased later, at $T = 1300$ K, which was caused by a greater adhesion of the metal to the substrate. The volume energy of the metal corresponds to the binding energy of the considered element. The experimental value of this energy at $T = 300$ K for nickel is equal to –4.44 eV/atom [17]. The close value of U_{Ni-Ni} (–4.39 eV/atom) for the nickel fcc crystal was obtained from the molecular dynamics calculation in an NPT ensemble [18]. The energy U_{Ni-Ni} calculated for the Ni_{23} cluster by the molecular dynamics method using the Sutton–Chen potential is equal to –3.70 eV/atom [19]. The energy U_{Ni-Ni} for a highly stretched nickel film at the considered temperatures has even higher values.

A further heating leads to an increase in the energy U_{Ni-Ni} for both systems. This increase is especially pronounced after the temperature of 2300 K for system I and after the temperature of 1800 K for system II. The dependence $U_{Ni-C}(T)$ for both systems exhibits a similar behavior, except that there is no decrease in the value of U_{Ni-C} upon the initial heating of system I and there is a rapid increase in the energy U_{Ni-C} for both systems after reaching a temperature of 1800 K. The potential energy for the free graphene sheet (in the absence of a metallic film) has the minimum at a temperature of 1800 K (curve *1* in Fig. 2b). The temperature dependences $U_{C-C}(T)$ for graphene in the presence of one and two films of the Ni atoms are completely identical (curve *2* in Fig. 2b). At lower temperatures ($T \le 1300$ K), the presence of a transition metal in the system stabilizes the graphene sheet, so that the energy U_{C-C} becomes lower than the energy of the free graphene sheet. This result is consistent with the data reported in [20], where it was shown that the stresses in graphene decrease after the graphene sheet is coated with nickel. The observed decrease in the energies U_{Ni-Ni} and U_{C-C} after contacting the graphene sheet and the nickel surface (including the nickel cluster) was explained in [21] by a significant attractive interaction between them. An increase in the temperature eventually leads to an increase in the potential energy. An increase in the graphene energy with increasing temperature in the presence of metal atoms occurs more rapidly (after 1300 K) than in their absence. The energy U_{C-C} at $T = 3300$ K for systems I and II is 4% higher than that for the free graphene sheet.

The temperature relaxation of stresses in the nickel films is illustrated in Fig. 3. It can be seen from this figure that each of the stresses σ_{zx}, σ_{zy}, and σ_{zz} decreases with an increase in the temperature. In the case where the graphene sheet is covered by one metallic film, it experiences very weak stresses, among which the stress σ_{zz} has the highest value. The strong interaction of nickel films with graphene in system II leads to the development of significant stresses in the film plane. The absolute values of the stresses acting in the *xy* plane are always higher in the lower film than in the upper film. This is caused by the smaller thermal stability of the lower film because of the rise of the atoms

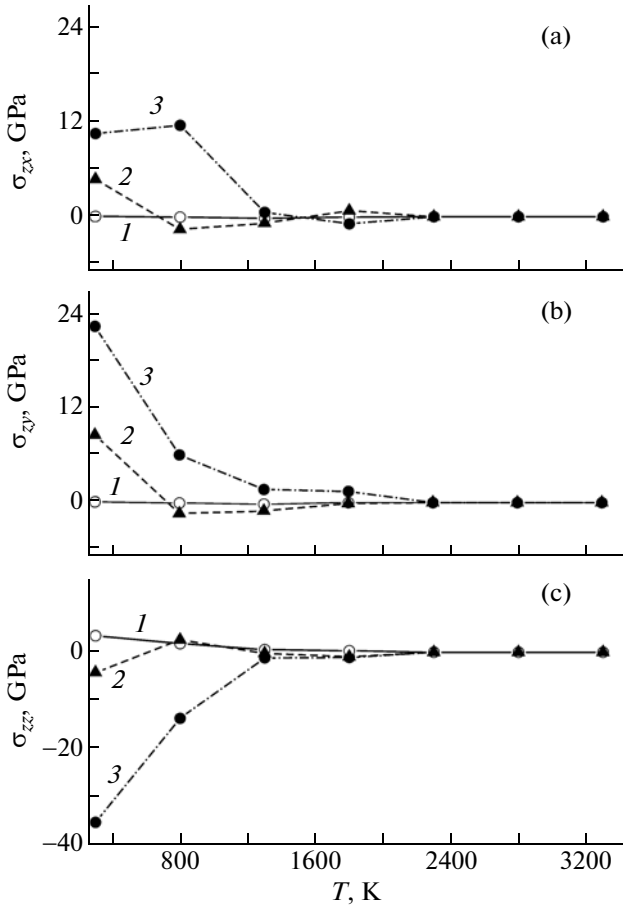

Fig. 3. Thermal relaxation of the stresses (a) σ_{zx}, (b) σ_{zy}, and (c) σ_{zz} in the plane of nickel films: (*1*) Ni film on one side of the graphene sheet, (*2*) upper Ni film on the graphene sheet with the two-sided coverage, and (*3*) lower Ni film on the graphene sheet with the two-sided coverage.

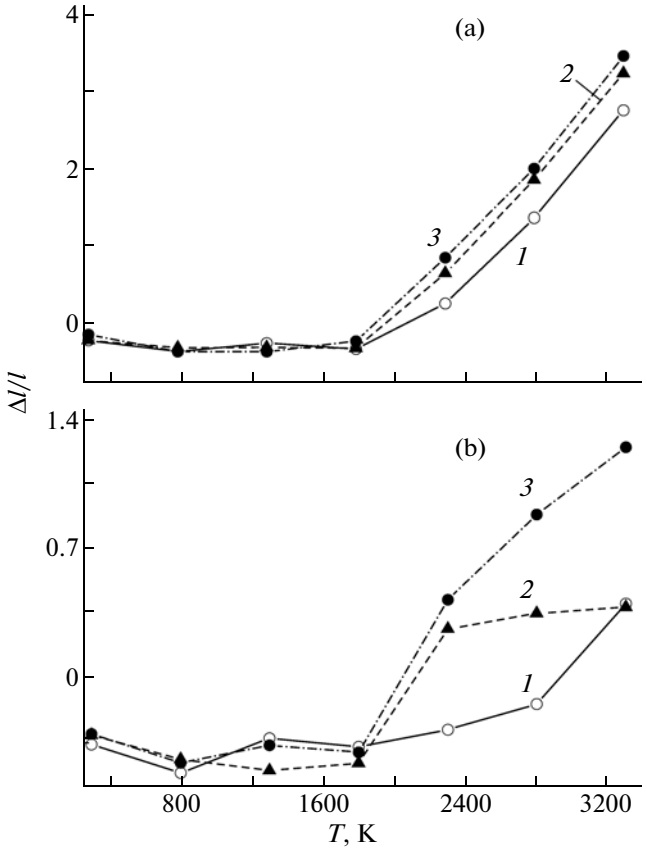

Fig. 4. Temperature dependences of the elongation per unit length of the nickel films on the graphene surface (a) in the "zigzag" direction and (b) in the "armchair" direction for (*1*) Ni film on one side of the graphene sheet, (*2*) upper Ni film on the graphene sheet with the two-sided coverage, and (*3*) lower Ni film on the graphene sheet with the two-sided coverage.

of the upper film. Owing to the long-range interaction in the metal, the atoms of the upper film, which rise with increasing temperature, "drag" the Ni atoms of the lower film, which, meeting the impermeable graphene, change their direction of motion and acquire higher velocities. Their further interaction with the lower lying atoms destroys the film. The initial minimum distance between the Ni atoms in different layers is almost 2.7 times longer than the distance between the nearest neighbors in the bulk metal. Already at the initial temperature (300 K), the stresses σ_{zz} in both the upper and lower metallic films have negative values, which is associated with a significant convergence of the metal atoms with the graphene separating the two nickel films. The positive value of σ_{zz} at $T = 300$ K for system I in the presence of one Ni film on graphene indicates that, in this case, there is no strong attraction of the Ni atoms to the graphene sheet; i.e., the Ni atoms have a looser packing.

The degree of divergence of the Ni atoms in the horizontal direction can be estimated from the temperature dependence of the elongation per unit length of the film in the directions of the axes *ox* and *oy* (Fig. 4). At temperatures below 1800 K, a small effective decrease in the sizes of the films (in the cases of the one and two films on graphene) is observed in both directions. This is caused by the instability of the stretched metallic structures. Consequently, during the heating, the Ni atoms are pulled together into more compact planar structures. At higher temperatures, the horizontal lengths of the films increase, and the value of $\Delta l/l$ for a single film increases more slowly than that for each of the films in the case of the two-sided coating of the graphene. The increase in the elongation $\Delta l/l$ is caused not only by the thermal expansion, but also by the melting of the films. Recall that the melting temperature of bulk solid nickel is equal to 1726 K. According to the molecular dynamics calculation using the Sutton–Chen potential, the melting temperature of the fcc Ni_{336} cluster is equal to 980 K, whereas the Ni_{8007} cluster melts already at 1380 K [22]. In all the considered cases, the Ni films

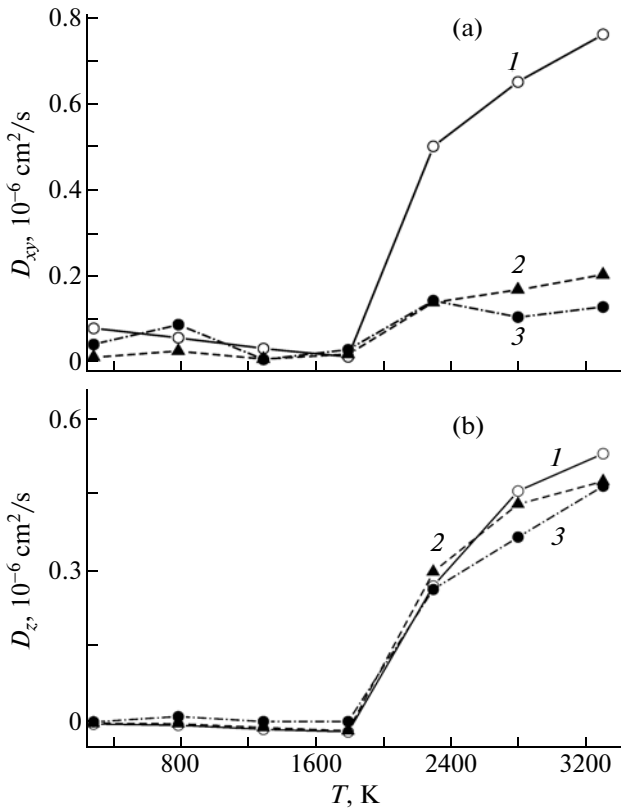

Fig. 5. Temperature dependences of the self-diffusion coefficient of nickel films on the graphene surface during the displacement of the Ni atoms in the (a) horizontal directions and (b) vertical direction for (*1*) Ni film on one side of the graphene sheet, (*2*) upper Ni film on the graphene sheet with the two-sided coverage, and (*3*) lower Ni film on the graphene sheet with the two-sided coverage.

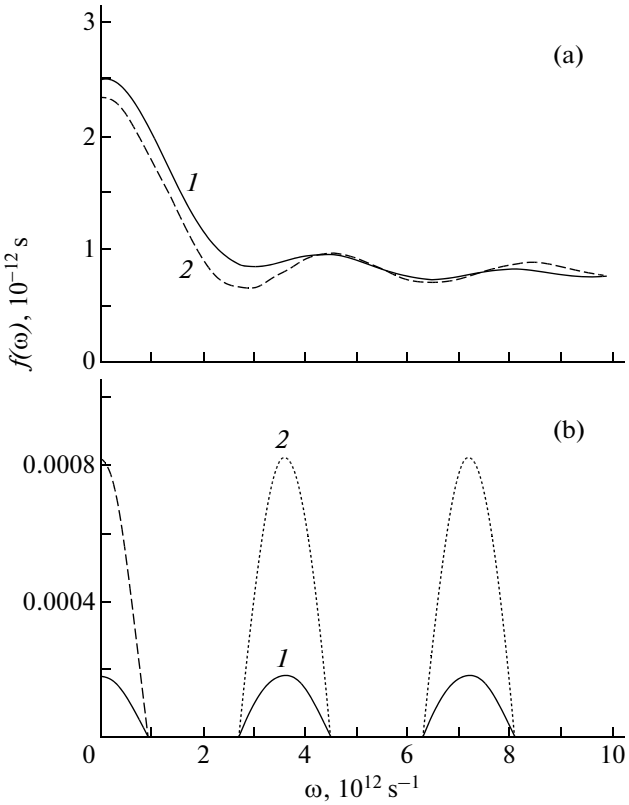

Fig. 6. Spectra of individual vibrations of the Ni atoms in thin films on the graphene surface during the displacement of the atoms in the (a) horizontal directions and (b) vertical direction for (*1*) Ni film on one side of the graphene sheet and (*2*) Ni films on both sides of the graphene sheet.

are most strongly expanded along the *ox* axis, which coincides with the "zigzag" direction in graphene. For example, in the case of the single-sided coating of graphene, the quantity $\Delta l/l$, which characterizes the Ni film, increases along this direction by a factor of almost four as compared to the corresponding characteristic in the direction *oy* with increasing temperature from 1800 to 3300 K. In the same temperature range, the value of $\Delta l/l$ for the lower Ni film of the two-sided coating of graphene in the direction *oy* increases, on the average, twice as fast as the corresponding characteristic for the upper film or the Ni film of the single-sided coating.

The self-diffusion coefficient of the Ni films for both the horizontal (D_{xy}) and vertical (D_z) directions varies very slightly to a temperature of 1800 K. This is associated with the conservation of the connectivity of atoms in the films, as well as with the densification of the structure at moderate temperatures. However, the coefficients of mobility of the atoms in different directions significantly increase after the temperature of 1800 K (Fig. 5). It is worth noting that the most significant increase in the coefficient D_{xy} is observed for the Ni film covering the graphene sheet on one side. This is associated with the weak influence exerted by graphene on the Ni atoms of the single-sided coating at high temperatures. The metal atoms, which interact through the graphene sheet, mutually inhibit their own horizontal displacements. The increase in the coefficient D_{xy} of the Ni atoms for system I, on the average, exceeds the corresponding characteristic for the upper and lower metallic films of system II by a factor of 5.7. A more similar behavior is observed for the self-diffusion coefficient D_z in the vertical directions for the Ni films in the single-sided and two-sided coatings of the graphene sheet. At the highest temperature (3300 K), the displacements of atoms in the vertical direction are still more preferred in the case of the single-sided coating. In each case, graphene offers resistance to the movement of the Ni atoms from only one side, and the metal atoms that interact through the graphene sheet weakly hold each other from the removal from the sheet in the vertical direction.

The temperature of 1800 K is critical in the fracture of nickel coatings on graphene. The spectra of individual vibrations of the atoms $f(\omega)$ for the Ni films at this temperature are shown in Fig. 6. The atomic vibrations in the horizontal direction are represented by the

continuous spectrum $f_{xy}(\omega)$, whereas the vibrational spectra of the Ni atoms in the vertical direction $f_z(\omega)$ consist of separate bands. The spectra $f_{xy}(\omega)$ for single- and double-sided nickel coatings are close enough in shape and amplitude. The spectra $f_z(\omega)$ for these film coatings have significantly different intensities, which differ by a factor of ~3.5–4.5. The characteristic frequencies for the spectra $f_z(\omega)$ of different nickel coatings remain unchanged. The vibration with a zero frequency dominates in the spectra $f_{xy}(\omega)$ over the two other most probable vibrations. Such vibrations are also strongly pronounced in the spectra $f_z(\omega)$. The presence of vibrations of the translational type in the vibrational spectrum indicates a liquid-like character of the atomic motion. The characteristic vibrations with a nonzero frequency in the spectra $f_z(\omega)$ have a red shift ($\sim 1 \times 10^{12}\ s^{-1}$) with respect to the corresponding vibrations in the spectra $f_{xy}(\omega)$. It is known that the shape of the vibrational spectra depends on the physical state of the substance, which provides information about the structure of different condensed phases. The spectra $f_z(\omega)$ have the type of absorption spectra of free molecules, whereas the spectra $f_{xy}(\omega)$ are defined as the spectra of disordered condensed phases. The vibrational properties of nickel films on graphene combine the corresponding properties of a disordered condensed phase and a gas, which is revealed from consideration of the vibrational spectra in different directions.

4. CONCLUSIONS

The heating of nickel films on single-layer graphene with single-sided and two-sided coverages of the graphene sheet with Ni atoms has been investigated using the molecular dynamics method. The partial potential energies U_{Ni-Ni} and U_{Ni-C} for these systems are rather close to each other, respectively. The presence of one metallic film on single-layer graphene has the same effect on the energy state of the graphene sheet as the presence of two metallic films on it. Moreover, the change in the energy of graphene covered by a metallic film with respect to the energy of a free graphene sheet has an alternating character. The maximum difference between these energies is observed at a temperature of 3300 K. The stresses generated in the Ni films for the system with the two-sided coverage of the graphene sheet are substantially higher than those for the single-sided coverage of the graphene. These stresses decrease with increasing temperature and reach the minimum even at a temperature of 1800 K. It is above this temperature that a significant increase in the elongation per unit length of the films in the "zigzag" and "armchair" directions of the graphene sheet begins to occur with a substantially stronger effect in the presence of metallic films on both sides of the sheet. The self-diffusion coefficient, which characterizes the displacement of the Ni atoms in the horizontal and vertical directions, also increases at temperatures above 1800 K. Furthermore, in the horizontal directions, the steepest increase in the coefficient of mobility of the Ni atoms is observed for the single-sided metallic film. The vibrational spectra of flat nickel–graphene systems have a continuous character for horizontal displacements of the Ni atoms and are discrete for vertical atomic displacements. The intensity of the bands in the spectrum significantly increases in the presence of the second Ni film on the reverse side of the graphene sheet.

REFERENCES

1. X. S. Li, W. Cai, J. An, S. Kim, J. Nah, D. Yang, R. Piner, A. Velamakanni, I. Jung, E. Tutuc, S. K. Banerjee, L. Colombo, and R. S. Ruoff, Science (Washington) **324**, 1312 (2009).
2. K. S. Kim, Y. Zhao, H. Jang, S. Y. Lee, J. M. Kim, K. S. Kim, J. H. Ahn, P. Kim, J. Y. Choi, and B. H. Hong, Nature (London) **457**, 706 (2009).
3. J. Wintterlin and M. L. Bocquet, Surf. Sci. **603**, 1841 (2009).
4. M. Moors, H. Amara, T. V. de Bocarme, C. Bichara, and F. Ducastelle, ACS Nano **3**, 511 (2009).
5. M. Eizenberg and J. M. Blakely, Surf. Sci. **82**, 228 (1979).
6. V. K. Portnoi, A. V. Leonov, S. N. Mudretsova, and S. A. Fedotov, Phys. Met. Metallogr. **109** (2), 153 (2010).
7. J. Kwak, J. H. Chu, J.-K. Choi, S.-D. Park, H. Go, S. Y. Kim, K. Park, S.-D. Kim, Y.-W. Kim, E. Yoon, S. Kodambaka, and S.-Y. Kwon, Nat. Commun. **3**, 645 (2012).
8. J. Tersoff, Phys. Rev. B: Condens. Matter: Condens. Matter **37**, 6991 (1988).
9. J. Tersoff, Phys. Rev. B: Condens. Matter: Condens. Matter **39**, 5566 (1989).
10. A. E. Galashev, Russ. J. Phys. Chem. B **6** (3), 441 (2012).
11. A. E. Galashev and O. R. Rakhmanova, High Temp. **51** (1), 97 (2013).
12. S. J. Stuart, A. V. Tutein, and J. A. Harrison, J. Chem. Phys. **112**, 6472 (2000).
13. H. Rafii-Tabar, Phys. Rep. **325**, 239 (2000).
14. M. Moseler, F. Cervantes, S. Hofmann, G. Csanyi, and A. C. Ferrari, ACS Nano **4**, 7587 (2010).
15. Z. Xu and M. J. Buehler, J. Phys.: Condens. Matter **22**, 485301 (2010).
16. H. J. C. Berendsen, J. P. M. Postma, W. F. van Gunsteren, A. DiNola, and J. R. Haak, J. Chem. Phys. **81**, 3684 (1984).
17. S. Erkoc, Int. J. Mod. Phys. C **11**, 1013 (2000).
18. T. Cagin, Phys. Rev. B: Condens. Matter **59**, 3468 (1999).
19. S. K. Nayak, S. N. Khanna, B. K. Rao, and P. Jena, J. Phys. Chem. A **101**, 1072 (1997).
20. H.-Y. Song and X.-W. Zha, Commun. Theor. Phys. (Beijing, China) **54**, 143 (2010).
21. Y. Shibuta and J. A. Elliott, Chem. Phys. Lett. **472**, 200 (2009).
22. Y. Qi, T. Cagin, W. L. Johnson, and W. A. Goddard III, J. Chem. Phys. **115**, 385 (2001).

Translated by O. Borovik-Romanova